

6-2010

Dielectrophoretic Separation of Mouse Melanoma Clones

Ahmet C. Sabuncu
Old Dominion University

Jie A. Liu
Old Dominion University

Stephen J. Beebe
Old Dominion University, sbeebe@odu.edu

Ali Beskok
Old Dominion University

Follow this and additional works at: https://digitalcommons.odu.edu/bioelectrics_pubs

 Part of the [Biomedical Engineering and Bioengineering Commons](#)

Repository Citation

Sabuncu, Ahmet C.; Liu, Jie A.; Beebe, Stephen J.; and Beskok, Ali, "Dielectrophoretic Separation of Mouse Melanoma Clones" (2010). *Bioelectrics Publications*. 45.
https://digitalcommons.odu.edu/bioelectrics_pubs/45

Original Publication Citation

Sabuncu, A.C., Liu, J.A., Beebe, S.J., & Beskok, A. (2010). Dielectrophoretic separation of mouse melanoma clones. *Biomicrofluidics*, 4(2), 021101. doi: 10.1063/1.3447702

Dielectrophoretic separation of mouse melanoma clones

Ahmet C. Sabuncu,¹ Jie A. Liu,^{2,3} Stephen J. Beebe,² and Ali Beskok^{1,a)}

¹*Department of Aerospace Engineering, Old Dominion University, Norfolk, Virginia 23529, USA*

²*Frank Reidy Research Center for Bioelectrics, Norfolk, Virginia 23508, USA*

³*The Department of Biology, Old Dominion University, Norfolk, Virginia 23529, USA*

(Received 16 February 2010; accepted 17 May 2010; published online 16 June 2010)

Dielectrophoresis (DEP) is employed to differentiate clones of mouse melanoma B16F10 cells. Five clones were tested on microelectrodes. At a specific excitation frequency, clone 1 showed a different DEP response than the other four. Growth rate, melanin content, recovery from cryopreservation, and *in vitro* invasive studies were performed. Clone 1 is shown to have significantly different melanin content and recovery rate from cryopreservation. This paper reports the ability of DEP to differentiate between two malignant cells of the same origin. Different DEP responses of the two clones could be linked to their melanin content. © 2010 American Institute of Physics. [doi:10.1063/1.3447702]

I. INTRODUCTION

Dielectrophoresis (DEP) is the motion of polarizable particles in nonuniform electric fields. DEP has been extensively used for biological cell manipulations. There are several studies aimed to separate cells by DEP, such as isolation of human leukemia,¹ stem,² breast cancer,³ or malaria infected cells⁴ from blood. One recent study demonstrated the use of a DEP-based microfluidic system for efficient isolation of circulating tumor cells from blood and also showed that the isolated cells were viable and suitable for further analysis.⁵ In another study, platelets were separated from blood by DEP activated cell sorter that can perform size based flow-fractionation.⁶ In addition to cell separation, it has been shown that cell dielectric properties can be extracted by DEP. In one study, morphology changes in stimulated Jurkat T-cells were investigated by calculating the cell membrane capacitance from the DEP crossover frequency.⁷

In this study, we present a method that can differentiate between two malignant cells of the same origin, which differ from each other by small changes in their melanin content. This study is a precursor for future efforts on DEP separation of metastatic human melanoma cells using microfluidic platforms.

II. MATERIALS AND METHODS

A. DEP

DEP force arises when a dipole is in interaction with a nonuniform electric field. The time averaged DEP force is given as⁸

$$\langle \bar{F}_{\text{DEP}}(t) \rangle = 2\pi\epsilon_m R^3 \text{Re}[f_{\text{CM}}] \nabla E_{\text{rms}}^2, \quad (1)$$

where $\langle f(t) \rangle$ represents the time average of the function $f(t)$, ϵ_m is the real part of the permittivity of the medium, R is the particle radius, E_{rms} is the root mean square of the electric field, and f_{CM} is the Clausius–Mossotti (CM) factor. This factor states the effective polarizability of the particle, and it is given as⁸

^{a)} Author to whom correspondence should be addressed. Electronic mail: abeskok@odu.edu.

TABLE I. Dimensions and dielectric parameters of B16 cells (Ref. 9).

	Symbol	Value
Radius	a	10 ⁻⁵ m
Membrane thickness	t	5 × 10 ⁻⁹ m
Membrane conductivity	σ _m	10 ⁻⁷ S/m
Cytoplasm conductivity	σ _{cyt}	0.5 S/m
Membrane permittivity	ε _m	4.4 × 10 ⁻¹¹ A s/V m
Cytoplasm permittivity	ε _{cyt}	7.1 × 10 ⁻¹⁰ A s/V m

$$\tilde{f}_{CM}(\tilde{\epsilon}_p, \tilde{\epsilon}_m) = \frac{\tilde{\epsilon}_p - \tilde{\epsilon}_m}{\tilde{\epsilon}_p + 2\tilde{\epsilon}_m}, \quad (2)$$

where $\tilde{\epsilon} = \epsilon - i\sigma/\omega$; ϵ and σ are the permittivity and conductivity, respectively; ω is the angular frequency; p and m indices are for particle and medium.

As previously used by Gascoyne *et al.* (1997) for mammalian cells, we have utilized the single shell model to represent biological cells. This model approximates the cell's complex permittivity as⁸

$$\tilde{\epsilon}_p = \tilde{\epsilon}_m \left[\gamma^3 + 2 \left(\frac{\tilde{\epsilon}_{cyt} - \tilde{\epsilon}_m}{\tilde{\epsilon}_{cyt} + 2\tilde{\epsilon}_m} \right) \right] / \left[\gamma^3 - \left(\frac{\tilde{\epsilon}_{cyt} - \tilde{\epsilon}_m}{\tilde{\epsilon}_{cyt} + 2\tilde{\epsilon}_m} \right) \right], \quad (3)$$

where $\gamma = R/(R-t)$; t is the cell membrane thickness; m and cyt indices show the membrane and cytoplasm.

B. Numerical calculations

CM factors of B16 cells were computed using Eqs. (2) and (3). Cells were assumed as perfect spherical particles. This is a reasonable approximation as cells become nearly spherical after nonspherical adherent cells were harvested from the culture flask by trypsinization. Cell's dielectric data for simulation were taken from the work of Oblak *et al.* and shown in Table I. Although it is obvious that the dielectric data of the cells used in this study will differ from the literature values, the simulations provided an initial guess for the crossover frequency. In addition, CM factor simulations were employed to investigate the effect of the cytoplasm conductivity. A numerical simulation of electric field on castellated electrode geometry with arbitrary electric potentials was done using electromagnetic module of finite element modeling software COMSOL MULTIPHYSICS® (COMSOL AB, Stockholm, Sweden).¹⁰ Electrostatic limit is assumed for electric field simulations, and hence, Laplace's equation was solved for electric potential in two dimensions. In simulations, electric potentials were prescribed on electrode boundaries and side boundaries were taken as symmetric. Electric field was used to distinguish between the positive and negative DEP zones on the chip.

C. Clone isolation

B16F10 clones were grown in Dulbecco's Modified Eagle Medium, (ATCC, Manassas, VA) with 10% fetal bovine serum (FBS), 1% L-glutamine, and 1% penicillin-streptomycin in an incubator with 5% CO₂ and at 37 °C. For all the measurements done in this study, cells in log phase were harvested by trypsinization. Like all cancer tumors and cancer cells lines, B16F10 melanoma cells are a heterogeneous population of cells. In order to isolate different clones from this heterogeneous population, B16F10 cells were treated with ten pulses of 60 ns, 60 kV/cm electric field exposures. Afterward, treated cells were plated at limiting dilutions, grown until individual colonies could be isolated as clones using sterile glass cloning cylinders. From a total of 18 clones, five clones numbered 1–5 were analyzed in this study.

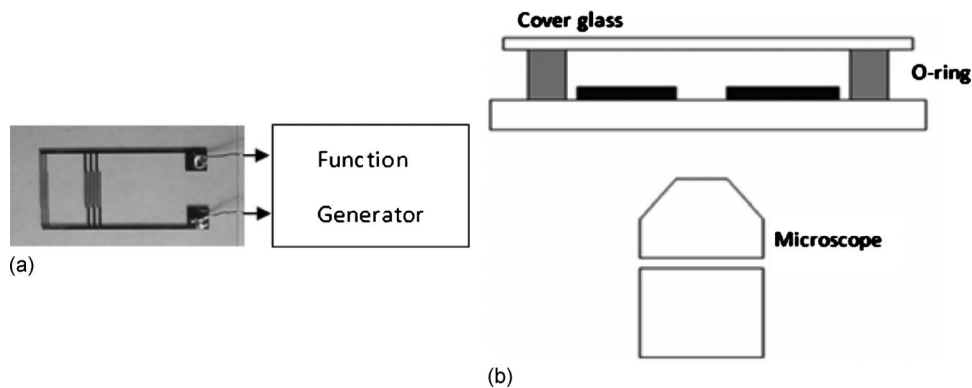


FIG. 1. (a) Two nontouching gold arrays were polarized by a function generator. Fluid and cell motions were observed by an inverted microscope. (b) Schematic view of the electrode array with a cover glass and O-ring on it.

D. DEP separation of clones

The cells were washed two times prior to DEP experiments with a cell manipulation buffer. The buffer consists of 8.6% (w/w) sucrose, 0.3% (w/w) dextrose, and 1.0 mg/ml Bovine Serum Albumin (Sigma-Aldrich, St. Louise, MO) and sufficient amount of modified eagle's minimum essential media (ATCC) to reach 0.16 S/m.⁷ The conductivity of the cell suspension media was measured by a conductivity meter (OMEGA, PHH-80PMS, Stamford, CT). The cell motion was observed under an inverted microscope (Olympus IX71, Cenmter Valley, PA) and at least three snapshots were taken at the steady state by a charge coupled device camera (Q Imaging, Surrey, BC, Canada). Cell counts in the results and discussion part were averaged over these snapshots. About 500 cells were counted at each frequency.

E. Microelectrodes

The microelectrodes were fabricated by using standard photolithography techniques. The experimental setup is shown in Fig. 1. The electrodes have characteristic dimension of 50 μm . The microelectrodes were energized by a function generator (BK Precision, Yorba Linda, CA) operating in sinusoidal mode.

F. Biological tests on clones

Melanin levels were determined from cell extracts as previously described by Kasraee *et al.*¹¹ and Kinoshita *et al.*¹² Briefly, 5.0×10^6 cells/ml cells were removed from the flask by trypsinization and dissolved in 1N NaOH. After 1 h incubation at 37 $^{\circ}\text{C}$, the solution was centrifuged and the absorbance of the extract was measured at 405 nm. The melanin amount was obtained from comparison to the standard curve of synthetic melanin (SIGMA, M8631). Cell invasion assay: Cultrex[®] BME cell invasion assay (R&D Systems, Cat No. 3455-096-K, Minneapolis, MN) was used to measure cell invasion through an extracellular matrix. Procedures were carried out in accordance with the manufacturer's recommendations. For growth rate measurements, cells were cultured in a complete medium in six-well plates for 24 h with a starting concentration of 0.1×10^6 cells/ml. After 24 h, cells were trypsinized and viable cell numbers were determined using a hemocytometer by exclusion of trypan blue. Assays were carried out in triplicate and experiments were repeated three times. Rate of recovery from cryopreservation was determined by freezing 1×10^6 cells in liquid nitrogen for 36 h. To determine viable cell numbers, these cells were thawed and cultured in 25 cm^2 cell flasks. 28 h later, viable cell numbers were determined using a hemocytometer by exclusion of trypan blue. The cell number was divided by 28 to determine the increase in cell number per hour. Assays were carried out in triplicate and experiments were repeated three times.

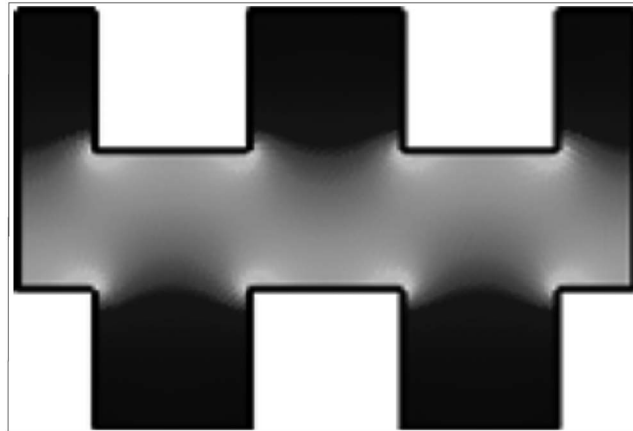


FIG. 2. Numerical simulation of electric field generated by castellated microelectrodes. Darker and lighter zones correspond to lower and higher electric field regions, respectively.

III. RESULTS AND DISCUSSION

A. DEP response and melanin content

The electric field simulation of castellated electrode is shown in Fig. 2, where the low and high electric field intensities correspond to darker and lighter regions, respectively. From Eq. (2), a cell with a positive CM factor will move toward the lighter zones (positive DEP). Likewise, a cell with a negative CM factor will travel toward darker zones. DEP separation of five B16F10 clones was tested under the applied electric potential of $5 V_{p.p.}$ at 200, 300, and 400 kHz frequencies. The response of clone 1 at 300 kHz was opposite of the other four clones. In the rest of this study the behavior of clone 1 is compared to that of clone 2, which was chosen randomly from the remaining four clones. In Fig. 3, final positions of cells on the chip are shown. At 200 kHz both clones showed negative DEP responses. However, as the frequency was increased the two clones showed different crossover frequencies from negative to positive DEP. At 300 kHz, clone 1 exhibited negative DEP, whereas clone 2 showed positive DEP. At 400 kHz, both clones showed positive DEP. Figure 4 shows the cell count of positive DEP response of B16 clones normalized by the total number of cells at three different frequencies. The results are obtained by counting the positive responses at each captured image and by dividing these to the total number of cells within the same image. At 200 kHz, most of the clone 1 cells show negative DEP response, while 25% of clone 2 cells show positive DEP. By 300 kHz, 90% of clone 2 cells and 20% of clone 1 cells show positive DEP response. The normalized count ratios differ significantly at 300 kHz, which indicates that the clones' DEP responses are almost opposite at this frequency.

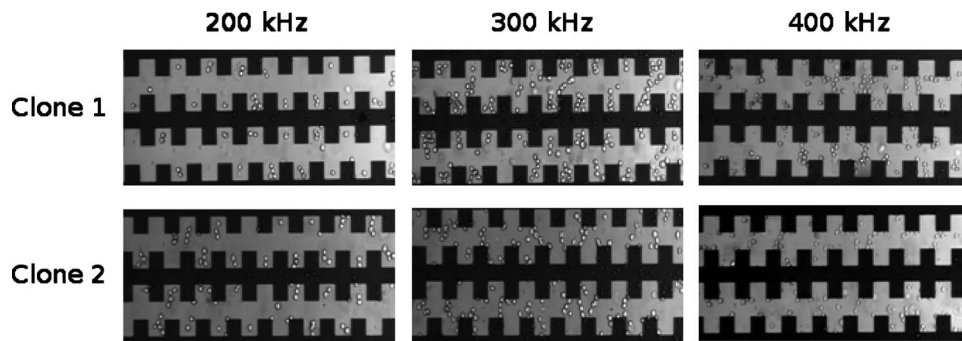


FIG. 3. Dielectrophoretic behavior of clones 1 and 2 under different excitation frequencies. Crossover frequency of clone 1 is found between 300 and 400 kHz; for clone 2 it is between 200 and 300 kHz. Applied voltage is $5 V_{p.p.}$.

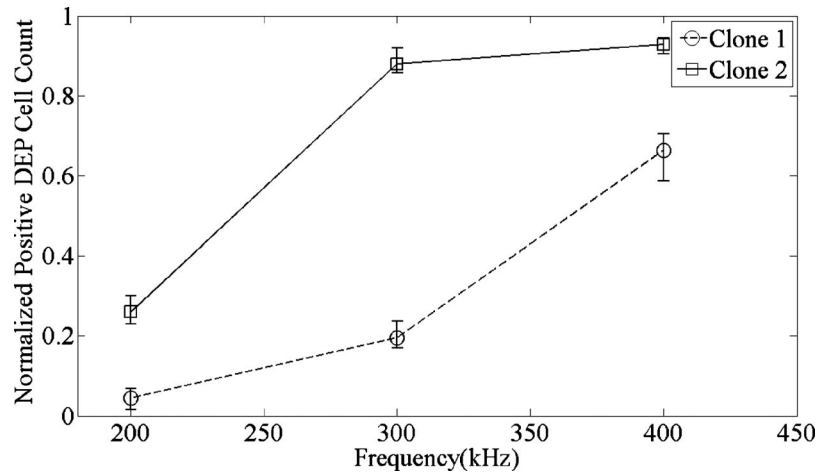


FIG. 4. Normalized cell count of B16 clones. The ratio is calculated as DEP positive cells divided by total number of cells.

In order to determine if these clones exhibited functional differences, further investigations were performed on B16F10 clones 1 and 2, including growth rates at normal conditions, recovery from cryopreservation, *in vitro* invasive capability, and melanin content. Among these tests for the two clones, normal growth rate, which is a measure of cell proliferation and invasion capability, which is an *in vitro* measure of metastasis, did not show significant difference (Table II). Thus, within the B16F10 heterogeneous population, which is an invasive cell line, both clones are equally proliferative and invasive. The rate of recovery from cryopreservation, which is a measure of recovery from extreme temperature stress, was very near the cutoff to be significant, and the melanin content was significantly different between the two clones. After melanin extraction, the absorbance at 405 nm of clone 1 was significantly higher than the absorbance of clone 2, with the p value being 0.001 (Table II). Interestingly, the rate of recovery from cryopreservation tended to be slower for the clone with the highest melanin content. Different melanin contents might also explain the different crossover frequencies of the two clones. Conductivity of melanin is lower than the conductivity of the cytoplasm.¹³ An increase in the percentage of melanin in cytoplasm may lead to a decrease in overall polarizability of the cell. In Fig. 5, we utilized the single shell model based on the data given by Oblak *et al.*, and varied only the σ_{cyt} value to investigate the effect of increased melanin content in cell cytoplasm. We varied the cytoplasm conductivity in between 0.3 and 0.6 S/m, based on the data given by Pethig (2006).¹⁴ The DEP crossover frequency increases by decreasing the cytoplasm conductivity, which may explain the different crossover frequencies observed in Figs. 3 and 4. It is worth noticing that the crossover frequency in Fig. 5 is based on the dielectric cell properties given by Oblak *et al.*, and starts at 400 kHz for $\sigma_{\text{cyt}} = 0.5$ S/m, while our experiments have shown the crossover frequency between 200 and 400 kHz. This slight mismatch could be induced by the differences in the original B16F10 cell line. In addition, the clones can be different in terms of their membrane properties, which also affect the CM factor.

TABLE II. Biological tests on B16 clones.

	Clone 1	Clone 2	P value
Melanin absorbance ^a (A405)	0.342	0.227	0.001 ^a
Rate slope recovery from cryopreservation (10^6 cell/h)	0.108	0.18	0.056
Growth rate slope (10^6 cell/h)	0.036	0.044	0.398
Invasion percentage (%)	2.63	2.62	0.99

^aRepresents statistical significance.

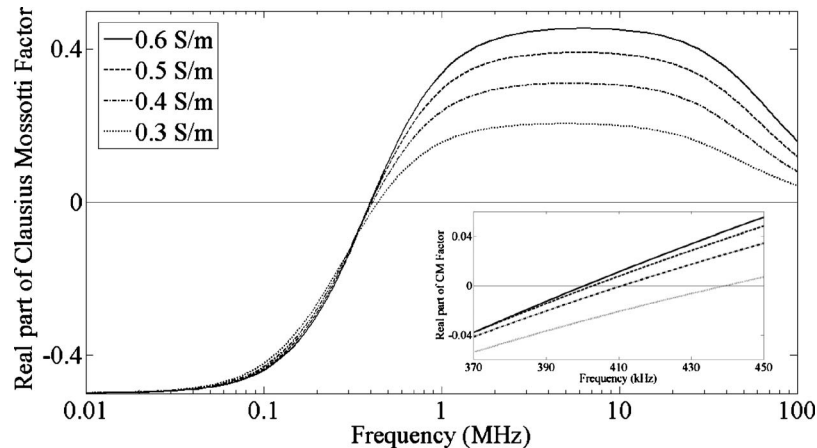


FIG. 5. Real part of CM factor of B16 cells at $\sigma_m=0.5$ S/m calculated from the dielectric data taken from the work of Oblak *et al.* (2007). The inset figure shows the change in the real part of CM factor between 370 and 450 kHz.

Since the cancer cell genomes are unstable, it is possible that these two melanoma clones may differ in ways other than their melanin content, which could explain the differences in their crossover frequencies. However, these two clones did not deviate in growth rate, they were not significantly different in recovery from cryopreservation and they did not vary in invasive capabilities. Each one of these functions requires hundreds of gene products, suggesting that the genomes of these clones were not significantly different. Based on these results, we suggest that the difference in the melanin content of these clones is most likely responsible for the differences in their crossover frequency.

IV. CONCLUSIONS

In this study, the capability of DEP to separate two B16F10 clones is presented. Clones 1 and 2 have significantly different melanin content. In contrast to other studies, which separate malignant cells from their healthy counterparts,¹⁻⁵ this study focuses on separating two malignant cells that have the same origin but differ in melanin content. The difference in the melanin content can be connected to increased MC1 (melanocortin-1 hormone)/MC1 receptor system, which is suggested to play a role in melanoma progression.¹⁵ While *in vitro* growth rates and invasion capacities of these clones were found to be similar, they do not specifically determine metastatic potential. Therefore, it might be inferred that differences in melanin content may determine metastatic potential of these clones and other melanomas, and DEP could be utilized to differentiate between these cells. Consequently, this study can be extended to a DEP-based microfluidic device that can separate malignant cells having different metastatic levels.

ACKNOWLEDGMENTS

This work was supported by the ODU Office of Research. We thank Ms. Sandy Anderson for isolation of B16F10 clones. The authors would like thank to Dr. Bayram Celik for the numerical simulations. A.C.S. and J.A.L. contributed equally to the work presented here.

¹F. F. Becker, X. B. Wang, Y. Huang, R. Pethig, J. Vykoukal, and P. R. C. Gascoyne, *J. Phys. D: Appl. Phys.* **27**, 2659 (1994).

²M. S. Talary, K. I. Mills, T. Hoy, A. K. Burnett, and R. Pethig, *Med. Biol. Eng. Comput.* **33**, 235 (1995).

³P. R. C. Gascoyne, X. B. Wang, Y. Huang, and F. F. Becker, *IEEE Trans. Ind. Appl.* **33**, 670 (1997).

⁴P. Gascoyne, C. Mahidol, M. Ruchirawat, J. Satayavivad, P. Watcharasil, and F. F. Becker, *Lab Chip* **2**, 70 (2002).

⁵P. R. C. Gascoyne, J. Noshari, T. J. Anderson, and F. F. Becker, *Electrophoresis* **30**, 1388 (2009).

- ⁶M. S. Pommer, Y. Zhang, N. Keerthi, D. Chen, J. A. Thomson, C. D. Meinhart, and H. T. Soh, *Electrophoresis* **29**, 1213 (2008).
- ⁷R. Pethig and M. S. Talary, *Inst. Eng. Tech. Nanobiotechnol.* **1**, 2 (2007).
- ⁸H. Morgan and N. G. Green *AC Electrokinetics: Colloids and Nanoparticles* (Research Studies Press, Baldock, UK, 2002).
- ⁹J. Oblak, D. Krizaj, S. Amon, A. Macek-Lebar, and D. Miklavcic, *Bioelectrochemistry* **71**, 164 (2007).
- ¹⁰See: www.comsol.com for commercial finite-element package COMSOL.
- ¹¹B. Kasraee, A. Hügin, C. Tran, O. Sorg, and J. Saurat, *J. Invest. Dermatol.* **122**, 1338 (2004).
- ¹²M. Kinoshita, N. Hori, K. Aida, T. Sugawara, and M. Ohnishi, *J. Oleo Sci.* **56**, 645 (2007).
- ¹³T. Ligonzo, M. Ambrico, V. Augelli, G. Perna, L. Schiavulli, M. A. Tamma, P. F. Biagi, A. Minafra, and V. Capozzi, *J. Non-Cryst. Solids* **355**, 1221 (2009).
- ¹⁴R. Pethig, in *Encyclopedia of Surface and Colloid Science*, edited by S. Somasundaran (Taylor & Francis, Boca Raton, 2006), Vol. 3, p. 1728.
- ¹⁵R. Lazova and J. M. Pawelek, *Exp. Dermatol.* **18**, 934 (2009).